Pergamon

PII: S0021-8502(99)00563-7

www.elsevier.com/locate/jaerosci

J. Aerosol Sci. Vol. 31, No. 7, pp. 789–799, 2000

Printed in Great Britain
0021-8502/00/$ - see front matter

APPLICATION OF THE T-MATRIX METHOD TO THE MEASUREMENT OF ASPHERICAL (ELLIPSOIDAL) PARTICLES WITH FORWARD SCATTERING OPTICAL PARTICLE COUNTERS

Stephan Borrmann,*† Beiping Luo‡ and Michael Mishchenko§

*Institut für Chemie und Dynamik der Geosphäre (ICG-1), Forschungszentrum Jülich GmbH, Jülich, Germany
‡Max Planck Institut für Chemie, Mainz, Germany
§NASA Goddard Institute for Space Studies, New York, NY, USA

(*First received* 19 *July* 1999; *and in final form* 27 *October* 1999)

Abstract—The response of the FSSP-300 and MASP optical particle counters with forward scattering geometries has been numerically simulated adopting the T-matrix method in order to assess the instrumental properties when exposed to clouds of aspherical particles (here: rotationally symmetric ellipsoids). The resulting scattering cross sections as function of particle size are compared to Mie theory calculations for spherical particles of the same refractive index, scattering geometry, and light wavelength. Based on these T-matrix calculations the FSSP-300 instrument is found suitable for use in populations of aspherical particles with aspect ratios larger than 0.5, if various caveats are taken into consideration. From the T-matrix method new tables result, which relate the instrument's size bin limits to actual particle sizes for a given refractive index. Two data sets of measurements in a cirrus cloud and an aircraft contrail are reduced by means of these new assignment tables in order to demonstrate the applicability of the method to atmospheric clouds. This paper also discusses in detail the limitations inherent in the use of the T-matix method as replacement for the Mie theory calculations commonly adopted for the FSSP-300 type of instruments.

1. INTRODUCTION

For the detection and sizing of individual aerosol particles by forward scattering optical particle counters Mie theory calculations are commonly applied to invert the measured scattered light signals into actual particle sizes. The assumption inherent in these calculations is that the particle shape geometry is spherical and the refractive index is isotropic. For the atmospheric aerosol in the stratospheric background or volcanic enhancements this assumption is met as in most tropospheric liquid-phase clouds. However in cirrus clouds, aircraft contrails, in polar stratospheric clouds (PSC) of type 2, to a lesser degree also in PSCs of type 1 (see e.g. Borrmann *et al*., 1993), as well as many other atmospheric aerosols the particle shapes deviate from spheres. Especially in cirrus clouds not only large ice crystals (with sizes above 100 μm) are found in measurements, but also significant concentrations of ice particles smaller than 30 μm (Noone *et al*., 1993). This raises the need for the extension of optical particle counter measurements to aspherical particles of small to moderate sizes. In the context of satellite data retrievals and lidar applications the so-called transition-matrix method (T-matrix method; see e.g. Waterman, 1971; Mishchenko, 1991; Bohren and Singham, 1991; Mishchenko *et al*., 1999) has been applied to backscatter and extinction calculations for aspherical particles (Mishchenko and Sassen, 1998). In this paper we applied a modified T-matrix code version to the specific scattering geometry of the FSSP-300 (Forward Scattering Spectrometer Probe model 300; manufactured by Particle Measuring Systems Inc. in Boulder Co., U.S.A.) *in situ* instrument which covers particle size diameters roughly ranging from 0.4 to 23 μm. The instrument characteristics, its experimental performance, and error sources are described in detail by Baumgardner *et al.* (1992). The aspherical particles were approximated by assuming rotationally symmetrical ellipsoids with different axis ratios. The instrument's response to the exposure in randomly

† Author to whom correspondence should be addressed.

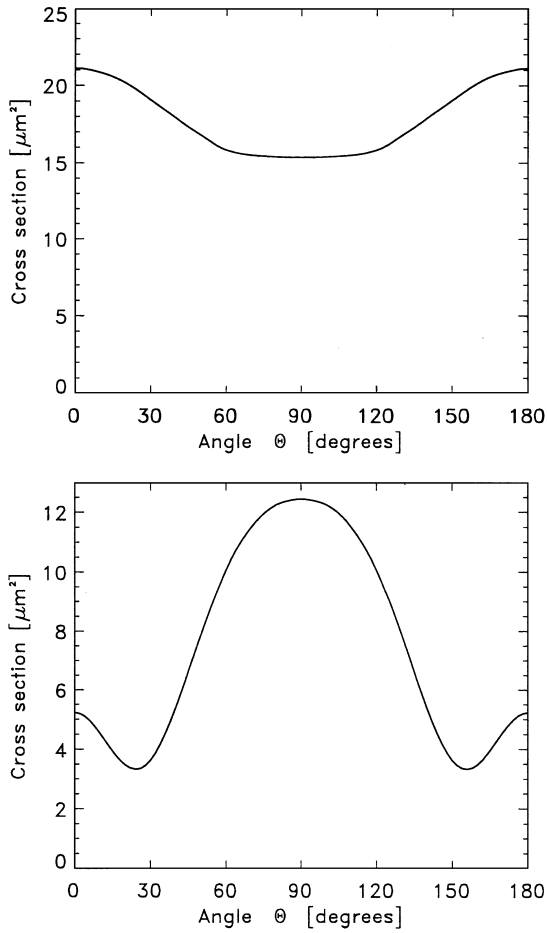

Fig. 1. Range of scattering cross sections as function of the orientation angle Θ covered by a 10 μm (upper panel) and a 4 μm (lower panel) diameter volume-equivalent ellipsoidal particle of 0.95 and 0.75 aspect ratio, respectively. The orientation angle is the angle Θ between the long axis of the particle and the incident laser beam for the FSSP-300 instrument geometry.

oriented ellipsoidal particle clouds are described in this paper together with examples of atmospheric measurements from a cirrus cloud and an aircraft contrail. Also described are exploratory results concerning the behavior of the newly developed MASP (Multi-Angle Spectrometer Probe; see Baumgardner *et al.*, 1996) when confronted with aspherical particles. Throughout the paper the limitations of the method are discussed in detail.

2. METHODOLOGY AND INSTRUMENT RELATED RESULTS

Both, Mie theory and T-matrix method, provide solutions of the Maxwell equations on the boundary conditions given by the experimental arrangement, the scattering objects, and the incident light. Mie theory provides closed solutions for spherical particles in a plane wave field, while the T-matrix method supplies numerical solutions for aspherical, but most often rotationally symmetric particles. For this work the small cirrus cloud particles were approximated by volume-equivalent, rotationally symmetric ellipsoids of different aspect (or axis length) ratios e. It was assumed that the scattered light signals received by the instrument were caused by a population of randomly oriented ellipsoids having an aspect ratio e. The upper panel in Fig. 1 shows the particle scattering cross section resulting from such T-matrix computations for rotationally symmetric ellipsoids of 10 μm volume-equivalent size diameter with an aspect ratio of $e = 0.95$ as function of the angle Θ between the incident laser beam and the particle's axis of rotational symmetry. For these numerical

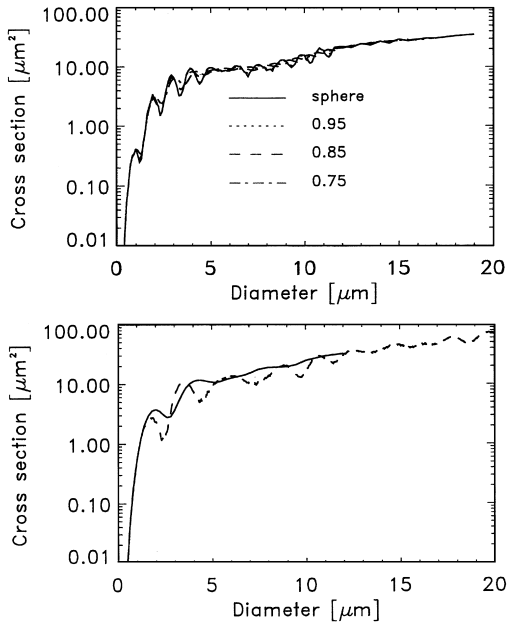

Fig. 2. The scattering cross sections for the FSSP-300 as function of particle size obtained from T-matrix calculations with averaging over all orientations. The upper panel shows the results for particles of different asphericities and a refractive index of $1.6 + 0.0i$, which is the refractive index of the polystyrene latex particles commonly used for instrument calibrations. The lower panel shows a comparison between Mie theory calculations (dashed line) and the T-matrix method (solid line) for (ice) particles of refractive index $1.31 + 0.00i$ having an aspect ratio of 0.5. Both panels are for HeNe laser light ($\lambda = 633$ nm) and the FSSP-300 scattering geometry (4–12°).

simulations the scattering geometry is that of the FSSP-300 (i.e., 4°–12° forward scattering angle range), the laser light wavelength is 633 nm, and the assumed particle refractive index is close to that of the polystyrene latex beads commonly utilized for the calibration of optical particle counters. The figure demonstrates the difference between the signals the instrument detector receives, if the particle is oriented parallel to the beam (angle $\Theta = 0$ or 180°), and if the particle is perpendicular to the beam (angle $\Theta = 90°$). Similarly, the lower panel in Fig. 1 displays results for a 4 μm diameter particle with an aspect ratio of 3:4, or $e = 0.75$. As expected is the maximum value of the scattering cross section for the 4 μm particle in the lower panel smaller than for the larger particle in the upper panel, but the functional relationship between Θ and the cross section is significantly different.

The upper panel of Fig. 2 shows the scattering cross sections of the particles as function of particle size (a so-called "response curve"), parameterized with respect to the axis lengths ratio e of the ellipsoids. The particle size diameters depicted at the abscissa correspond to those of volume-equivalent spheres. The cross sections for the aspherical particles (dotted, dashed, and dot-dashed lines) are obtained by subjecting a particle with given asphericity e to the T-matrix model a large number of times, where the orientation of the particle's long axis with respect to the direction of the incident laser beam is cycled through all angles. The output of the T-matrix code then is the average over all orientations. The solid line in the upper panel of Fig. 2 represents the T-matrix calculation for an "ellipsoid", which is degenerated to a sphere and this computation has to, and does, coincide with the results from Mie-theory calculations.

The lower panel in Fig. 2 shows the same kind of results of T-matrix calculations (solid line) up to 20 μm particle diameter, but for the refractive index of ice and an average aspect ratio of 0.5. These T-matrix calculations are complex, computing time intensive (requiring several hours of CPU time on a high end workstation), and the numerical algorithm becomes unstable at certain particle sizes dependent on the refractive index and the degree of asphericity. For example in the upper panel of Fig. 2 the method is unstable for particle

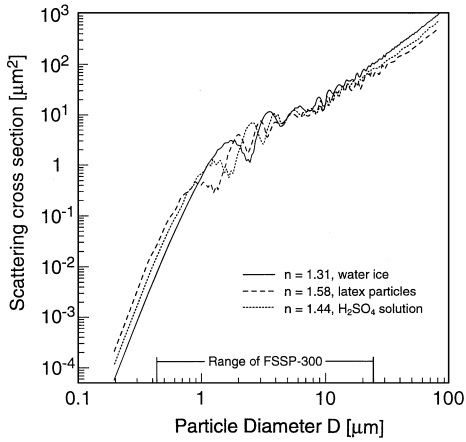

Fig. 3. Mie theory calculations of the scattering cross section as function of particle size for the refractive indices of ice, latex particles, and H_2SO_4 solution droplets for HeNe laser light and the scattering geometry of the FSSP-300.

diameters larger than 17 μm with an aspect ratio of 0.95. This "instability" size limit moves towards smaller sizes as the asphericity increases for a given wavelength. For asphericities between $e = 0.5$ and 0.75 typical upper-limit diameters are around 16 μm, if the so-called "LU factorization" method (Mishchenko *et al.*, 1999) is utilized. This extends over most of the particle size diameter range nominally covered by the FSSP-300. However, this upper stability limit is dependent on the scattering geometry of the instrument and the specific boundary conditions under investigation.

In the lower panel of Fig. 2 both methods show "bumps" in the scattering cross section for spherical particles around 1.5, 3.5, 6, ... μm diameter (see also Fig. 3). Thus, if the detector reports a measured scattering cross section of around 2 μm^2 (see lower panel of Fig. 3), then three possibilities arise for particle sizes, which could have caused the light signal corresponding to this scattering cross section. (Going right from the ordinate at 2 μm^2 in Fig. 3 one crosses the solid curve three times, each of which is associated with a different particle size on the abscissa. Which one of the three possible sizes actually caused the detected signal cannot be determined.) This so-called "Mie ambiguity" due to the "Mie resonant structure" constitutes one of the major disadvantages of the instrument configuration, because it is not possible to resolve the particle size in the region of such "bumps" (see e.g. Garvey and Pinnick, 1983 or Szymanski and Liu, 1986). One large particle size bin has to be created by the analysis software into which all detected scattered light reflexes from the ambiguity region are sorted. Even if the electronics of the instrument is capable of discriminating the signals originating from the photo-detector with a higher resolution, this resolution would have to be deteriorated in the analysis software to accomodate the effect of these Mie ambiguities. As demonstrated in Fig. 3, the problem is aggravated by the fact that the position of the response curve together with the Mie ambiguities varies considerably with the particle refractive index. For this reason it is so important to have (albeit difficult to obtain) an indication for the refractive indices of the particles encountered by the instrument for example during flight operation on a research aircraft. Otherwise, the location of the Mie ambiguities is unknown and it is difficult, if not impossible, to associate the detected light reflexes with the sizes of the scatterers. Interestingly, as the asphericity of the particle is increased (by decreasing the aspect ratio) the amplitudes of the Mie resonant structures decrease, as has been observed for forward scattering arrangements by Chylek *et al.* (1976). This reduces the extent of the ambiguity region on the abscissa and is tantamount to an improvement of the size resolution of the instrument (see dot-dashed lines in the upper panel and solid line in the lower panel of Fig. 2). However, this effect is accompanied by a significant disadvantage inherent in the requirements of counting statistics. To obtain a small error due to counting statistics, it suffices for spherical particles to count some fairly

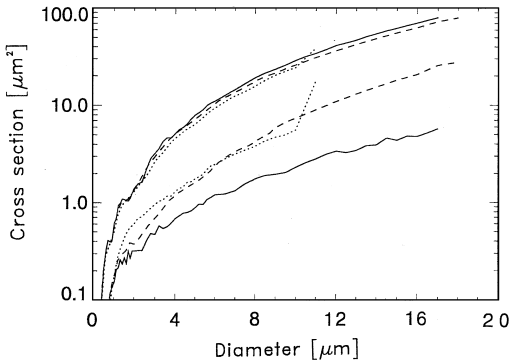

Fig. 4. Scattering cross sections for the multi-angle spectrometer probe (MASP) in forward direction (upper set of three curves) and backward direction (lower set of curves). The solid lines represent (spherical) particles with aspect ratio 1.0, the dashed lines refer to 0.75 aspect ratios, and the dotted lines to $e = 0.5$. The refractive index of the particles is 1.6, and the laser wavelength 732 nm.

large number of them into each size bin. For the rotationally symmetrical ellipsoids a large number of particles of *each orientation* must be counted into each size bin, because the method demands averaging over all orientations. Thus, a much larger total number must be sampled than in case of spherical particles. Depending on the desired accuracy with respect to counting statistics and depending on the particle size range and binning of interest, for a typical application of the FSSP-300 a total number of the order of 2000 particles needs to be detected per size distribution to accomodate for the increased requirements due to the different orientations of the passing particles. Also the method is limited to clouds where the crystals are randomly oriented in the air. This may not always be the case, as examples of certain kinds of haloes show, at least for larger ice particles. If, in an extreme case, all particles of some sampled population were "aligned", having the same orientation in the air, the resulting size distribution reported by the instrument would be wrong.

Based on these calculations the forward scattering geometry of the FSSP-300 allows for the use of the instrument in clouds of aspherical particles under the described assumptions. It is worthwhile noting that other scattering geometries of optical particle sizing instruments may exhibit different features in the response curves. The MASP is designed to simultaneously collect the light scattered from an individual particle in two independent angular cones: in forward direction between 29° and 61°, and in backward direction between 119° and 151° (Baumgardner *et al.*, 1996). Figure 4 displays the T-matrix results for these two directions for different particle asphericities, for diode laser light of 732 nm, and a particle refractive index of 1.6. The upper set of three lines is the scattering cross section of the forward cone, the lower set corresponding to the backward direction. The differences between the lower three lines (note the log scale axis) demonstrate the potential of this instrument for differentiating between particles of different asphericities based on the back-scattered light signal. Note also that the onset of the numerical instability region of the T-matrix method can be seen at 10 μm where the curves abruptly bend upwards.

3. APPLICATION TO CIRRUS CLOUD MEASUREMENTS

The FSSP-300 nominally covers the particle size diameter range from approximately 0.4 to 23 μm with 31 size bins. The particle size diameters associated with the upper and lower limits of each of these 31 bins are calculated once based on a response curve from Mie theory for the refractive index of ice (1.31), and a second time adopting a response curve from the T-matrix method for the same refractive index. This response curve was computed assuming a lognormal distribution of aspect ratios around a mean e of 1:2, because it cannot be expected that all atmospheric particles detected for a measurement with the FSSP-300 have precisely the same value for e (see below the discussion of Fig. 5). Therefore, a narrow lognormal distribution having $\sigma = 1.2$ was used. The resulting bin limit sizes for

Table 1. Bin limit sizes for the FSSP-300 particle counter from T-matrix calculations for the refractive index of ice (1.31) assuming particles having a mean aspect ratio of 1:2 and a lognormal distribution around this mean with a sigma of $\sigma = 1.2$

Bin number	Lower bin limit size diameter (μm)	Upper bin limit size diameter (μm)	Combined bin number
1	0.374	0.444	1
2	0.444	0.496	2
3	0.496	0.547	3
4	0.547	0.598	4
5	0.598	0.646	5
6	0.646	0.695	6
7	0.695	0.743	7
8	0.743	0.890	8
9	0.743	0.890	8
10	0.890	0.939	9
11	0.939	0.976	10
12	0.976	1.059	11
13	1.059	1.137	12
14	1.137	1.252	13
15	1.252	1.394	14
16	1.394	2.816	15
17	1.629	3.081	15
18	3.081	3.266	16
19	3.266	3.446	17
20	3.446	3.670	18
21	3.670	3.935	19
22	3.935	5.789	20
23	5.789	6.444	21
24	6.444	7.043	22
25	7.043	7.517	23
26	7.517	8.549	24
27	8.549	10.07	25
28	10.07	11.26	26
29	11.26	12.67	27
30	12.67	14.13	28
31	14.13	15.77	29

both methods are shown in Tables 1 and 2 in a similar way to those given by Baumgardner *et al.* (1992) for other refractive indices of spherical particles. The first column in the tables contains the "house" numbers of the bins of the FSSP-300 as delivered (and hardwired through a chain of resistors preceding the pulse height analysis) by the manufacturer. The second and third columns give the lower and upper size diameters in μm for these bins and the given refractive index. The last column shows "combined bins" because due to the ambiguities in certain size ranges nominal bins of column 1 need to be combined together. For example in Table 1 there are two rows labelled "15" in the last column. Due to the Mie ambiguities the corresponding two bins from column 1, namely number 16 (having lower and upper bin limit sizes 1.394 and 2.816) and 17 (with bin limits 1.629 and 3.081), overlap and for particles between 1.629 and 2.816, for example, it is not possible to determine into which bin they belong. Therefore bins number 16 and 17 of the original bin configuration in column 1 need to be combined to this new bin number 15 from column number 4, which then has the lower and upper limits of 1.394 and 3.081 μm. Evading Mie ambiguities by creating new wider bins out of the narrower original bins this way decreases the size resolution of the instrument considerably. Comparing Tables 1 and 2 it becomes evident that the size resolution (i.e., the number of combined bins in column 4) is larger for the T-matrix method than for the Mie theory calculations. Due to the smaller amplitudes of the Mie resonance structures originating from the T-matrix result the size resolution is improved. (Note: The identical bin limits for parts of Tables 1–3 result from two circumstances: (1) The threshold voltages for the 31 bins in columns 1 were hardwired by the manufacturer. (2) The bin limits for the indicated refractive index were obtained from the original calibration at refractive index 1.58 for polystyrene latex.) Similar bin limits can be

Table 2. Bin limit size diameters for the FSSP-300 from Mie theory calculations for spherical particles with a refractive index of 1.31 for ice

Bin number	Lower bin limit size diameter (μm)	Upper bin limit size diameter (μm)	Combined bin number
1	0.380	0.430	1
2	0.430	0.480	2
3	0.480	0.520	3
4	0.520	0.570	4
5	0.570	0.610	5
6	0.610	0.650	6
7	0.650	0.700	7
8	0.700	0.840	8
9	0.840	0.890	9
10	0.890	0.930	10
11	0.930	0.960	11
12	0.960	1.050	12
13	1.050	1.120	13
14	1.120	2.730	14
15	1.120	2.730	14
16	1.120	2.730	14
17	1.120	2.730	14
18	2.730	4.940	15
19	2.730	4.940	15
20	2.730	4.940	15
21	2.730	4.940	15
22	4.940	7.080	16
23	4.940	7.080	16
24	7.080	10.04	17
25	7.080	10.04	17
26	10.04	11.07	18
27	11.07	11.35	19
28	11.35	13.28	20
29	13.28	13.57	21
30	13.57	21.41	22
31	13.57	21.41	22

deduced for other refractive indices such as in Table 3 for nitric acid trihydrate of type 1 polar stratospheric clouds with 1.483.

Figure 5 shows a comparison between Mie theory and T-matrix method for the particle size distribution measured by the ER-2 on 16 January 1989. Inside a cirrus cloud (Borrmann *et al*., 1996) the FSSP-300 delivered particle count results for its 31 size bins. The data in Fig. 5, show the particle size distributions resulting for the two different techniques, where for the T-matrix method a mean aspect ratio of $e = 1:2$ (with $\sigma = 1.2$) was assumed. These are arbitrary assumptions at this point as no data indicating the degree of asphericity of these natural particles were available. The axis ratio of 1 : 2 covers the "most aspherical" geometry for which the numerical solutions converge, at the same time extending over almost the entire nominal size range of the instrument. However, in a cirrus cloud with a size distribution similar to that of Fig. 5 Ström *et al.* (1997) collected crystal replica samples which indicate that this $e = 1:2$ assumption seems very reasonable. Since particles with well-defined edges and corners are absent in their sample, the replica photograph in Ström *et al.* (1997) additionally demonstrates that the assumption of rotationally symmetric ellipsoids underlying these T-matrix calculations is met by a significant number of ice particles in the size range below 20 μm. Ohtake (1970) suggested that such "droxtals" result from rapid freezing of haze droplets where the formation of hexagonal shapes is inhibited. As pointed out by Solomon *et al.* (1997), it is mainly these small ice particles which possibly play a major role for the heterogeneous chemistry in the tropopause region. In Sassen *et al.* (1995) pictures of Formvar-preserved cirrus ice crystals with sizes above 100 μm are shown which do exhibit the hexagonal and columnar shapes one usually associates with cirrus clouds.

Table 3. T-matrix calculations of the FSSP-300 bin limits for the refractive index of nitric acid trihydrate (1.483) in type 1 polar stratospheric clouds assuming lognormally distributed particle aspect ratios around a mean e of 0.5 with a σ of 1.2 as for Table 1

Bin number	Lower bin limit size diameter (μm)	Upper bin limit size diameter (μm)	Combined bin number
1	0.322	0.377	1
2	0.377	0.422	2
3	0.422	0.469	3
4	0.469	0.515	4
5	0.515	0.560	5
6	0.560	0.606	6
7	0.606	0.652	7
8	0.652	0.803	8
9	0.652	0.803	8
10	0.803	0.857	9
11	0.857	0.901	10
12	0.901	1.011	11
13	1.011	1.140	12
14	1.140	1.937	13
15	1.937	2.073	14
16	2.073	2.221	15
17	2.221	2.378	16
18	2.378	3.839	17
19	2.378	3.839	17
20	3.839	4.204	18
21	4.204	5.689	19
22	5.689	6.750	20
23	6.750	8.025	21
24	8.025	8.941	22
25	8.941	9.807	23
26	9.807	10.654	24
27	10.654	12.157	25
28	12.157	13.432	26
29	13.432	15.282	27
30	15.282	16.796	28
31	16.796	18.385	29

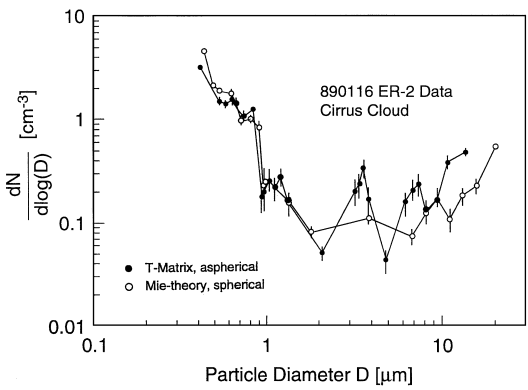

Fig. 5. Comparison of the cirrus cloud particle size distribution from 16 January 1989, measured by an FSSP-300 instrument: Mie theory versus T-matrix method (for lognormally distributed aspect ratios around a mean of 1 : 2 with a σ of 1.2). The particle refractive index is 1.31 for both curves. The error bars denote the uncertainties due to counting statistics based on counting a large number of particles only, and not counting a large number of different orientations (see text for details).

The higher size resolution of the T-matrix method becomes evident in Fig. 5 near 1 μm, and in the 2–9 μm size range. Both methods agree relatively well for particles smaller than 2 μm, which is to be expected, because for such small particles the asphericities do not have a large effect. Application of the T-matrix curve for the refractive index of ice (1.31) to the 31 bin limits results in an upper detection limit (i.e., the upper size diameter of bin number 31 in

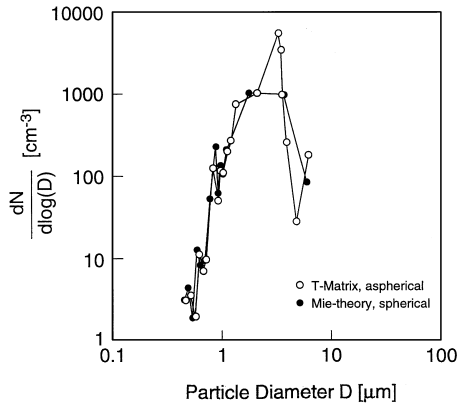

Fig. 6. Comparison of the ice particle size distribution from 15 March 1996, measured by the University of Mainz/Forschungszentrum Jülich FSSP-300 in an aircraft contrail at cruising altitude: Mie theory versus T-matrix method (for aspect ratios of 1:2 and $\sigma = 1.2$). The particle refractive index is 1.31 for both curves.

Table 1) of 15.77 μm for the FSSP-300. Utilizing the corresponding Mie response curve for spherical particles instead yields an upper size limit for bin number 31 of 21.41 μm. In other words, the instrument "sees" only particles with size diameters between 0.38 and 21.41 μm, if the response curve from Mie theory (1.31 refractive index) is adopted, while the same particle population would be reported as having sizes between 0.37 and 15.77 μm, if the analysis software uses the T-matrix result for the same refractive index. For these reasons a quantity like the total aerosol surface area delivered by the two methods for Fig. 5 can differ by more than a factor of two, despite the fact that the total number of particles detected per cm^3 of air is the same for both methods (i.e. 0.9 particles per cm^3). If the size detection range of the FSSP-300 for the Mie response curve is truncated artificially at approximately 16 μm to match with the upper detection limit of the T-matrix method, then the surface areas resulting from both methods are closer (within a factor of 1.3 for this specific example) to each other. It is this last (combined) size bin (number 22 in the fourth column of Table 2) between 13.57 and 21.41 μm, which contributes most of the surface area for the Mie based result in Fig. 5. For this refractive index the T-matrix method becomes numerically unstable at particle sizes larger than the FSSP-300's upper size limit of 16 μm diameter. At other refractive indices the method could become unstable at sizes inside the instrument's range, which has to be taken into account when assigning sizes to bin limits.

In Fig. 6 results are displayed from measurements in an aircraft contrail (Petzold *et al.*, 1997). The FSSP-300 of the University of Mainz/Forschungszentrum Jülich was carried on the DLR Falcon research aircraft into the contrail a few hundred meters behind an ATTAS passenger airplane at 9300 m cruising altitude on 15 March 1996. For the smallest particles the curves resulting from Mie theory and the T-matrix method are similar, while they differ for sizes larger than 1 μm. Again the T-matrix method yields a higher size resolution for the sizes above 1 μm.

4. CONCLUSIONS

The main conclusions from the numerical study of the scattering behavior of aspherical particles in an FSSP-300 instrument are:

1. It is possible to use the FSSP-300 in clouds of particles where the assumption of rotationally symmetric ellipsoids seems justified.

2. From T-matrix calculations based on the response curves for different refractive indices new tables can be generated, which associate the upper and lower size limits of each of the 31 size bins of the FSSP-300 to the corresponding scattering cross sections. These size limits differ from those resulting from Mie theory. A higher size resolution is obtained with

the T-matrix method, if one considers the Mie ambiguities in the 0.8–8 μm diameter range. For the refractive index of ice the FSSP-300 covers a size diameter range from 0.4 to 21.4 μm, if Mie theory is used, and from 0.37 to 15.77 μm, if the T-matrix method is adopted with a mean asphericity of 1 : 2 and a lognormal distribution around this mean having a $\sigma = 1.2$.

3. The derived surface areas obtained by Mie theory are roughly a factor of 2 higher compared with the T-matrix method. This factor is only valid for the cirrus cloud events analyzed in this study, and will be different in case of other refractive indexes and asphericities. Caveats concerning the counting statistics especially in the large particle region of the FSSP-300 size range, need to be taken into account.

The first conclusion is not obvious, as it was frequently thought that the application of an FSSP-300 in cirrus clouds is not possible, and it was necessary to prove the instrument's feasability for the cirrus cloud measurements. This applies to the FSSP model 300 only, because T-matrix method currently is not useful for cirrus clouds where a large fraction of the particles is greater than roughly 20 μm in diameter. One reason for this is the numerical instability of the computational algorithm for larger sizes. However, application of the T-matrix code adopting the LU factorization procedure (as suggested by Mishchenko *et al.*, 1999) may allow to compute instrument response functions extending well into the range of the FSSP-100 thus covering larger particle sizes. But even then care needs to be exercised with respect to the validity of approximation of cirrus particles as ellipsoids.

Conclusion (2) is the quantitative basis for reducing the measured data from cirrus clouds to obtain estimates for the particiulate surface area values, which is necessary for example for studies of heterogeneous chemistry in cirrus clouds.

A few more items need to be included in this discussion:

1. For the modelling of small cirrus cloud crystals/particles by rotationally symmetrical ellipsoids the question arises exactly which aspect ratio needs to be utilized and what the variation of the aspect ratios within a cirrus particle population is.

2. The influence of the width σ of the lognormal aspect ratio distribution on the response functions requires more detailed studies.

3. The higher size resolution resulting from the T-matrix calculations may be partially offset by possible "crosstalk" (i.e. the counting of large particles into size bins for smaller particles in cases where the laser beam intercepts the large particle at its smallest area cross section). This point needs further theoretical and experimental study.

4. Other T-matrix calculations were performed replacing the ellipsoids by rotationally symmetric cylinders. The results do not drastically differ from those for ellipsoids.

5. Further limitations regarding the experimental conditions for the deployment of FSSP type instruments inside cirrus or mixed phase clouds may apply as described in Gardiner and Hallett (1985).

Due to its forward scattering geometry and its coverage of small particle sizes the FSSP-300 seems suitable for measurements in cirrus clouds with small ice crystals. This is also the case for PSC type 1 and 2 clouds since the particles encountered there mostly are small enough for the inherent assumptions to hold (Borrmann *et al.*, 1993).

Acknowledgements—We gratefully acknowledge the help of Dr Andreas Petzold and Franz Schröder (Institute for Physics of the Atmosphere, DLR, Oberpfaffenhofen, Germany) for the data handling of the contrail measurements on the DLR Falcon. This research was partially financed by the EU Environment and Climate Program under contract ENV4-CT93-0352, and by the German BMBF under contract 01LO9310.

REFERENCES

Baumgardner, D., Dye, J. E., Gandrud, B. W. and Knollenberg, R. G. (1992) Interpretation of measurements made by the Forward Scattering Spectrometer Probe (FSSP-300) during the Airborne Arctic Stratospheric Expedition. *J. Geophys. Res.* **97,** 8035–8046.

Baumgardner, D., Dye, J. E., Gandrud, B. W., Barr, K., Kelly, K. K. and Chan, K. R. (1996) Refractive indices of aerosols in the upper troposphere and lower stratosphere. *Geophys. Res. Lett.* **23,** 749–752.

Bohren, C. F. and Singham, S. B. (1991) Backscattering by nonspherical particles: a review of methods and suggested new approaches. *J. Geophys. Res.* **96,** 5269–5277.
Borrmann, S., Dye, J. E., Baumgardner, D., Wilson, J. C., Jonsson, H. H., Brock, C. A., Loewenstein, M., Podolske, J. R. and Ferry, G. V. (1993) *In-situ* measurements of changes in stratospheric aerosol and the N_2O–aerosol relationship inside and outside of the polar vortex. *Geophys. Res. Lett.* **20,** 2559–2562.
Borrmann, S., Solomon, S., Dye, J. E. and Luo, B. (1996) The potential of cirrus clouds for heterogeneous chlorine activation. *Geophys. Res. Lett.* **23,** 2133–3136.
Chylek, P., Grams, G. W. and Pinnik, R. G. (1976) Light scattering by irregular randomly oriented particles. *Science* **193,** 480–482.
Gardiner, B. A. and Hallett, J. (1985) Degradation of in-cloud forward scattering spectrometer probe measurements in the presence of ice particles. *J. Atmos. Oceanic Technol.* **2,** 171–180.
Garvey, D. M. and Pinnick, R. G. (1983) Response characteristics of the Particle Measuring Systems Active Aerosol Spectrometer Probe (ASASP-X). *Aerosol Sci. Technol.* **2,** 477–488.
Mishchenko, M. I. (1991) Light scattering by randomly oriented axially symmetric particles. *J. Opt. Soc. Am. A* **8**(6), 871–882.
Mishchenko, M. I. and Sassen, K. (1998) Depolarization of lidar returns by small ice crystals: an application to contrails. *Geophys. Res. Lett.* **25,** 309–312.
Mishchenko, M. I., Travis, L. D. and Macke, A. (1999). T-matrix method and its applications. In *Light Scattering by Nonspherical Particles*: *Theory*, *Measurements*, *and Applications*, (Edited by Mishchenko, M. I., Hovenier, J. W. and Travis, L. D.), pp. 147–172. Academic Press, San Diego.
Noone, K. B., Noone, K. J., Heintzenberg, J., Ström, J. and Ogren, J. A. (1993) In situ observations of cirrus cloud microphysical properties using the counterflow virtual impactor. *J. Atmos. Oceanic Technol.* **10,** 294–303.
Ohtake, T. (1970) Unusual crystals in ice fog. *J. Atmos. Sci.* **27,** 509–511.
Petzold, A., Busen, R., Schröder, F. P., Baumann, R., Kuhn, M., Ström, J., Hagen, D. E., Whitefield, P. D., Baumgardner, D., Arnold, F., Borrmann, S. and Schumann, U. (1997) Near field measurements on contrail properties from fuels with different sulfur content. *J. Geophys. Res.* **102,** 29,867–29,880.
Sassen, K., Starr, D. O. C., Mace, G. G., Poellot, M. R., Melfi, S. H., Eberhard, W. L., Spinhirne, J. D., Eloranta, E. W., Hagen, D. E. and Hallett, J. (1995) The 5–6 December 1991 FIRE IFO II jet stream cirrus case study: possible influences of volcanic aerosols. *J. Atmos. Sci.* **52,** 97–123.
Solomon, S., Borrmann, S., Garcia, R. R., Portman, R., Thomason, L., Poole, L. R., Winker, D. and McCormick, M. P. (1997) Heterogeneous chlorine chemistry in the tropopause region. *J. Geophys. Res.* **102,** 21,411–21,429.
Ström, J., Strauss, B., Anderson, T., Schröder, F., Heintzenberg, J. and Wendling, P. (1997) In situ observations of the microphysical properties of young cirrus clouds. *J. Atmos. Sci.* **54,** 2542–2553.
Szymanski, W. W. and Liu, B. Y. H. (1986) On the sizing accuracy of laser optical particle counters. *Part. Charact.* **3,** 1–7.
Waterman, P. C. (1971) Symmetry, unitarity, and geometry in electromagnetic scattering. *Phys. Rev. D* **3,** 825–839.